



# Series elastic actuation for improved transparency in time delayed haptic teleoperation<sup>☆</sup>

Daniel Budolak, Pinhas Ben-Tzvi<sup>\*</sup>

Robotics and Mechatronics Lab, Department of Mechanical Engineering, Virginia Tech, Blacksburg, VA 24060, USA

## ARTICLE INFO

### Keywords:

Teleoperation  
Time delay  
Haptics  
Series elastic actuation (SEA)

## ABSTRACT

This paper demonstrates that incorporating passive compliance to the follower (slave) by means of a series elastic actuator (SEA) improves system transparency for haptic teleoperation applications with large time delays. Time delay induced force and position tracking errors limit the practical implementation of teleoperation systems. Traditional approaches have focused on passifying the communication channel and estimation methods to improve transparency, but performance degrades in large delays. In a force-position architecture using a Smith predictor, the ability to implement force control through position control with an SEA aids in increasing transparency of the system. The position drift common in most time delayed systems is eliminated with the proposed method while maintaining an accurate force reflection for a constant round trip time delay of two seconds. The combined actuation and sensing capabilities of the SEA also provide a means for detecting and correcting for variations in the environment contact location. This aids in estimating the follower dynamics for the predictor as both position and force information of the environment are captured. The proposed method is validated through simulation and experiment involving stiff and soft unilateral environment contact. The results of haptic teleoperation with an SEA demonstrate the effectiveness of compliance for accurate system transparency and improved performance in comparison to stiff actuation, while reducing controller complexity.

## 1. Introduction

While teleoperation has been studied for quite some time, the practicality of time delayed systems has been significantly improved in recent years. A survey by [1] reviews contemporary control approaches to extend the capabilities of time delayed haptic systems. Many of the most recent methods are built off of earlier control architectures that are presented in a historical survey by [2]. Improving time delayed haptic teleoperation continues to be important work, as it is the most suitable solution when a human operator is desired but unavailable due to a remote or hazardous environment. Applications for this include space, subsea, robotic surgery, nuclear/disaster sites, and virtual reality [1,2]. The majority of approaches to extend teleoperation performance in greater time delays has been done with focus on passifying the communication channel, and application of control schemes that estimate the environment and follower dynamics. Although some achieve good force tracking performance, position error and performance losses in larger delay times is often reported. This paper rethinks the approach by examining the mechanical system and investigating environment contact dynamics, proposing the use of passive compliance through an SEA for extending teleoperation performance.

The remaining sections are organized as follows: **Section 2** reviews the state of the art. **Section 3** defines the problem being addressed and elaborates on the proposed solution. **Section 4** provides a detailed discussion and formulation of the teleoperation system. **Sections 5** and **6** provide the simulation and experimental results with discussion respectively. Finally, **Section 7** gives concluding remarks and presents future work.

## 2. Literature review

Previously, increasing the performance and ensuring stability of teleoperation systems has been addressed using model based predictive approaches augmented with estimators and adaptive methods [3,4], or additions such as neural networks (NN) [5,6], wave variables [7,8], energy bounding approaches (EBA) [9,10] or optimization [11]. Oftentimes, a Smith predictor (SP), first proposed in [12], will be implemented as the main controller, although other model based predictors have also been studied. In this scheme, if the time-delayed dynamics are perfectly predicted then the time delay is canceled out.

The greatest challenge in predictive control approaches is obtaining an accurate model or estimation of the follower and environment, particularly when the follower and environment dynamics are nonlinear or

<sup>☆</sup> This paper was recommended for publication by Associate Editor Dr Denny Oetomo.

<sup>\*</sup> Corresponding author.

E-mail addresses: [dbudolak@vt.edu](mailto:dbudolak@vt.edu) (D. Budolak), [bentzvi@vt.edu](mailto:bentzvi@vt.edu) (P. Ben-Tzvi).



Fig. 1. 2-Channel force position teleoperation system. \* denotes delayed signal.

time varying. To address this [5] uses an online NN to estimate follower side dynamics. As an online method, the network can respond to small changes in the follower and environment dynamics. However, the NN weights can take up to 1.5 s for a round trip time (RTT) delay of 500 ms to converge.

Others have addressed the concerns with predictive methods by using adaptive model based approaches in [4,11,13]. From the most recent example, the improved extended active observer in [13] relies on accurate rigid body models and observers to estimate the external and friction torques of the system. This approach, like most adaptive methods, can handle variations in the communication delay but is limited to small delay times, and its ability to adapt to varying environment dynamics has not been investigated.

Performance in teleoperation is based on transparency between the master and follower (slave) system. In early studies, transparency was focused on matching the impedance transmitted to the operator ( $Z_{to}$ ) to the environment impedance ( $Z_e$ ) such that  $Z_{to} = Z_e$ . A 4-Channel (4C) approach was proposed where both force and velocity signals are transmitted [14]. However, transparency was achieved at the expense of passivity. To guarantee passivity, the common two channel method was developed, but with a loss of transparency [15]. This asserts that transparency and passivity are opposing goals that researchers continue to combat. The two channel architecture is depicted in Fig. 1 where  $F$  and  $x$  denote the force and position signals, and subscripts  $h$ ,  $m$ ,  $f$ , and  $ref$  refer to the human, master, follower, and reflected value, respectively.

Passivity, as first presented for teleoperation systems with scattering variables by [16], is a convenient and conservative assurance of stability, and thus has been widely implemented through transformation variables applied to signals sent through the communication channel. The use of wave variables (WV) in particular has become very popular since it guarantees stability regardless of the time delay and follower side dynamics. However, because no position information is explicit, available position drift is a common consequence. A detailed discussion on the benefits and limitations of WV is presented in [17].

WV have also been notably used to stabilize the  $H_\infty$  controller in [8]. This study performed a pick and place telemanipulation task between the USA and Japan in an RTT of 0.48 s, with the help of voice queues from the follower side. Although this work successfully presented a practical demonstration, it was constrained to a small delay. Additionally, the system features the common performance and stability trade-off for passivity approaches.

An energy bounding approach (EBA) is another method used to achieve passivity without scattering or WV [9]. Here the concept of passivity is applied as a controller to bound energy output on both the master and follower. This method was expanded in [10] where the bilateral EBA was combined with an SP force position (F-P) architecture. Similar to [7] this method guarantees stability, but has the common stability-performance trade-off since the EBA bounds the force magnitude on the master side. Like many approaches, the predictive EBA also needs to know the environment dynamics to have good transparency. Alternatively, [18] used a sliding mode based finite time controller with a barrier Lyapunov function to address performance and stability, with a NN for uncertainties. This has promising results with its ability to constrain the position error, but has not been applied to environment interaction.

Earlier work in teleoperation has also investigated shared compliance control (SCC) [14]. It was recognized that compliance on the fol-

lower side is beneficial for safely controlling the remote robot. However, at the time, manipulator stiffness was preferred for positional accuracy. Thus, compliance was actively achieved through impedance control despite certain advantages of passive compliance. A well known example is the remote compliant center (RCC) wrists [19]. Because of this, passive compliance remains mainly unexplored in teleoperation, despite many potential benefits that can be applied in the form of an SEA.

SEA's have many advantages over direct drive actuators including accurate force control, and reduced force errors from friction and torque ripples that can cause position drift [20]. Moreover, the unified force through position control of SEAs lends itself very well to the F-P architecture in teleoperation. Compliant robots are also becoming increasingly more popular in both research and industry as safe human interaction is becoming a critical concern. The main method of ensuring safe operation is minimizing inertial forces and enforcing compliance by passive means with SEA's instead of active control, as compliant actuators lower the reflected inertia [20,21]. A new robot design in [22] showcases the importance and the benefits of passive joint compliance through SEA's in contact detection as well as unified force motion control.

Since an SEA functions as a force/torque sensor as well as an actuator, contact can be determined by measuring the joint torques while interacting with an unknown environment. This is beneficial for teleoperation as it provides a method to accommodate varying environments. A study by [23] also suggests that the use of SEA's on the follower side may be beneficial in future teleoperation systems. Another study [24] makes note that the effects of compliance in haptic feedback has not been examined thoroughly.

### 3. Methodology

To the knowledge of the authors, the practical limits for bilateral haptic teleoperation is an RTT of approximately 500 ms. Performance of teleoperation systems degrades as the delay time increases, particularly for systems that enforce passivity. Moreover, few studies have investigated robust solutions to varying environment dynamics. Much work remains for increasing haptic teleoperation performance in large time delays by further examining unexplored components of the system such as environment contact on the follower side. To address these issues this paper presents the novel use of an SEA as a compliant end effector on the follower side, for improved transparency in time delays of up to two seconds and adaptability to environment position variation, with a simplified control strategy.

The proposed system uses an F-P architecture with an SP to combat the effects of time delay. In this approach, the slave robot tracks a position command from the master device and sends back the external force from the environment, where it is reflected back onto the user by the master haptic device. Because the slave side tracks the master position, it is referred to as the follower. In this scheme transparency is achieved through position and force matching, such that  $x_h = x_e$  and  $F_h = F_e$ , where the subscripts  $h$  and  $e$  refer to the human operator and environment, respectively. Additionally, in the implementation of an F-P architecture, the reflected force becomes proportional to the follower position through the spring constant and thus the outer loop force control also drives the position tracking. This reduces the common deviation between force and position error and simplifies modeling of the follower-environment system. Due to the compliance and force position relationship, the system is far more robust to large time delays.

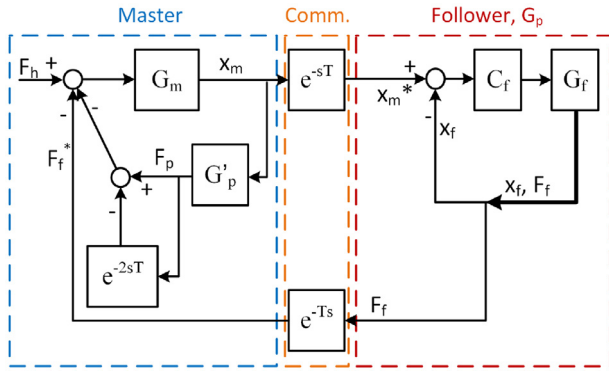


Fig. 2. Block diagram of the proposed force-position Smith predictor architecture.

Although time delays can be time varying and asymmetrical, methods to deal with the nonlinear and time-varying effects of internet communication have been studied in [25–28]. Moreover, time varying delays can be turned into constant delays with the use of buffering and a network delay regulation [27]. Because the proposed system can be applied in tandem with some of these methods, for simplicity of presenting the control strategy and to focus on the novelty of using an SEA, this study assumes a known constant delay.

#### 4. Teleoperation system

##### 4.1. Smith predictor

Due to its simplicity and proven performance, the Smith predictor is the primary method for dealing with time delay. In the Smith predictor, the desired force feedback  $F_p$ , can be written as

$$F_p = G'_p(1 - e^{-sT'})x_m + F_f \quad (1)$$

where  $G'_p$  is the follower dynamics estimate,  $T'$  is the estimated round trip time delay,  $x_m$  is the position of the master, and  $F_f$  is the actual force feedback from the follower side

$$F_f = e^{-sT}G_p x_m. \quad (2)$$

The desired reflected force can be rewritten in terms of the time delay and follower dynamics such that the equation becomes

$$F_p = G'_p(1 - e^{-sT'})x_m + e^{-sT}G_p x_m \quad (3)$$

where  $G_p$  is the actual follower dynamics and  $T$  is the round trip time delay. If the time delay is known,  $T' = T$ , and the follower dynamics are perfectly predicted,  $G'_p = G_p$ , then the time delay is canceled out and the reflected force becomes

$$F_p = G_p x_m. \quad (4)$$

Because no passivity enforcing control is applied to this architecture, the system is only stable when there is full cancellation of the time delayed dynamics,  $G_p = G'_p$ , with proper controller selection on the follower side. Thus, stability for the proposed system with the architecture presented in Fig. 2 is dependent on the accuracy of the follower and environment dynamics modeling. When modeling error is present, stability of the teleoperation system can still be guaranteed for a bounded error using Nyquist criteria [29]. From examination of the representative block diagram of an SP in Fig. 3, the closed loop transfer function is

$$G_{cl} = \frac{CGe^{-sT}}{1 + CG' + C\Delta Ge^{-sT}} \quad (5)$$

where  $\Delta G$  is additive modeling error. Based on the Nyquist theorem the system will be stable if  $1 + C(j\omega)G(j\omega) > C\Delta G(j\omega)e^{-j\omega T}$ . The additive

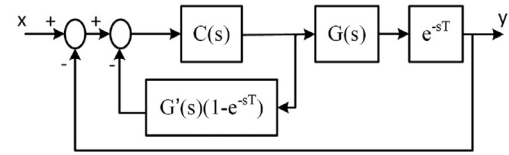


Fig. 3. General Smith predictor system with time delay.

error can be represented as  $G(j\omega)\delta G(j\omega)$ , where  $\delta G(j\omega)$  is multiplication modeling error. The stability condition now becomes

$$|1 + [C(j\omega)G(j\omega)]^{-1}| > |\delta G(j\omega)e^{-j\omega T}| \quad (6)$$

Thus,  $|\delta G(j\omega)| < W(\omega)$ , where  $W(\omega)$  is an upper bound function requiring

$$|1 + [C(j\omega)G(j\omega)]^{-1}| > W(\omega) \quad \forall \omega. \quad (7)$$

Therefore, even with modeling error the SP remains stable for the teleoperation system based on the appropriate selection of  $C$  for the follower dynamics. The stability of the presented architecture is verified in experiment.

##### 4.2. Compliance in the system

The addition of passive compliance to the follower provides many advantages for improving the capabilities of teleoperation systems. Compliance is beneficial because with two objects in contact, the kinematics of the most compliant member dominates. This becomes evident by examining the pole locations of both a stiff and compliant system. The time constant depends on the pole locations  $Re\{\lambda\}$ , where  $\lambda$  is an eigenvalue of the system.  $\lambda$ 's with large time constants decay quickly and only the compliant dynamics remain. Thus, if the follower has a compliant member such as an SEA in contact with the environment, where the follower impedance is much smaller than that of the environment,  $Z_f \ll Z_e$ , then the force exerted by the follower on the environment reduces to the SEA spring displacement as given by Hooke's Law. However, this simplification cannot be made with a stiff follower, or when the compliances have a similar relative order of magnitude. For these cases the environmental force is

$$F_e = \begin{cases} -K_s(x_e - x_f) & K_f \ll K_e \\ f(x_f, x_e, \dot{x}_e) & K_f \gg K_e, K_f \approx K_e \end{cases} \quad (8)$$

where  $K$  is stiffness with subscripts e, f, and s referring to the follower, environment, and SEA respectively, and  $f$  is a generalized function that is dependent on the follower position  $x_f$ , environment contact location  $x_e$ , velocity  $\dot{x}_e$ , and may be time-varying with linear or nonlinear stiffness and damping. Naturally, if  $K_f > K_e$  then the SEA will be unable to measure the contact force since the spring does not displace. For measuring environmental forces in this situation, a secondary force sensor can be used at the expense of stiff contact behavior common in F-P architectures. Thus, the spring stiffness must be appropriately selected for the environment and use case. Environment dynamics can also be nonlinear. With traditional SP approaches, nonlinear environment dynamics cause prediction errors that lead to transparency losses, thereby destabilizing the system. With an SEA, the environment position is known through contact with the follower and the position is encoded in the force signal. This is used to update the prediction model and allows the proposed system to have good force and position tracking even in contact with soft nonlinear environments.

The compliant follower is a great simplification in both the sensing and modeling of the follower and environment. Because SEA's decouple the inertia of links in a multi-link manipulator, only a single SEA in contact with the environment is presented. The generalized rotary model is formulated as a force sensing SEA similar to that examined by [30]. Including the electrical and mechanical subsystems, the SEA is modeled as follows. The electrical system is coupled to the motor dynamics by the motor torque, which is proportional to the current as  $\tau_m = K_m i$  with

motor constant  $K_m$ . The motor is coupled to the load by  $\tau_{out}$  through the spring displacement  $d_s = N^{-1}\theta_m - \theta_l$ , giving

$$\begin{aligned} Ri + L \frac{di}{dt} + K_m \dot{\theta}_m &= V \\ J_m \ddot{\theta}_m + B_m \dot{\theta}_m &= \tau_m - \tau_{out} \\ J_l \ddot{x}_l + B_l \dot{x}_l &= \tau_{out} + \tau_{ext} \\ K_s d_s &= \tau_{out} \end{aligned} \quad (9)$$

where  $J_l$  and  $B_l$  are the mass and damping of the load,  $J_m$  and  $B_m$  are the motor inertia and damping,  $V$  is the voltage applied to the motor,  $L$  is the armature inductance, and  $R$  is the armature resistance.

For the proposed linear actuator used in experiment, the rotary motion from the DC motor is converted into linear motion with a lead screw as  $x_m = N^{-1}\theta_m l / 2\pi$ , where  $l$  is the screw pitch. The force applied by the SEA is then  $F_{out} = K_s d$  where displacement  $d = x_m - x_l$ , and  $x_m$  and  $x_l$  are the motor and load positions. The general linear load dynamics now become  $M_l \ddot{x}_l + B_l \dot{x}_l = F_{out} + F_{ext}$ .

From the system of equations above, an open loop transfer function relating the output force of the SEA to the input voltage while the follower is in contact can be written as

$$\frac{F_{out}}{V} = \frac{K_s K_m l}{2\pi s[(Ls + R)(J_m s + B_m) + K_m^2]} \quad (10)$$

A PID control law can be applied to this for position control of the SEA for implementation of the proposed F-P architecture as follows:

$$\begin{aligned} e &= x_m - x_f \\ V &= k_p e + k_I \int e + k_D \dot{e}. \end{aligned} \quad (11)$$

Without loss of generality,  $x_f$  can be set to zero with  $x_m$  being the new set point relative to  $x_f$ . The transfer function for the follower side dynamics for use in calculating  $F_p$  in the SP is now

$$G_p = \frac{K_s K_m l (K_D s^2 + K_P s + K_I)}{2\pi s^2 [(Ls + R)(J_m s + B_m) + K_m^2]} \quad (12)$$

### 4.3. Environment contact location sensing and correction

Compensating for time varying environment dynamics is important for teleoperation systems with large time delays since prediction schemes in particular necessitate exact knowledge of the follower and environment dynamics. Generally, the follower side dynamics are assumed to be known a priori, and not subject to disturbances. In predictive architectures, inaccurate estimation will have losses in transparency from delay cancellations, and subsequently large force reflection error. Thus, any unknown environmental variations can lead to undesired collisions resulting in destabilizing oscillations or damage to the system and environment. Because the SEA is capable of both position and force sensing, it can be used to compensate for varying environment dynamics without the use of a neural network or an adaptive control scheme. For environment position variation, if there is an error in the environment contact location,  $F_p \neq F_f$  even if  $x_m = x_f$ . Because the force on the follower is proportional to the SEA spring displacement,  $x_e$  can be calculated by the difference in follower position and spring displacement as

$$x_e = x_f - \frac{F_f}{k_s}. \quad (13)$$

The spring displacement cannot be used directly since the F-P architecture only uses two channels to send and receive the position and force respectively. During operation when the environment position varies, the contact location  $x_e$  is determined from Eq. (13) upon initial contact with the environment, and the force reflection is carried out with the new estimate. This method continuously updates  $x_e$  while in contact with the environment.

**Table 1**  
Simulation parameters.

Parameter	Value
$J_m$	4 E-6 kg m <sup>2</sup>
$J_l$	2 E-4 kg m <sup>2</sup>
$B_m$	2.9 E-5 Nm s/rad
$B_l$	1.0 E-4 Nm s/rad
$K_s$	5 Nm/rad
$N$	10
$R$	4 $\Omega$
$L$	2.7 E-6 H
$K_m$	0.0275 Nm/ $\sqrt{W}$

## 5. Unilateral contact dynamics simulation

Often the initial contact dynamics are not considered in teleoperation since a stationary environment is passive from energy and momentum conservation of impact. However, this ignores important aspects of the system such as the large impulses that occur due to discontinuity in velocity upon impact. When these are large, the resulting oscillations can degrade performance, in particular for higher speeds. Perhaps since teleoperation was developed with a "move and wait" strategy in its formative years [2], most studies and applications have been low bandwidth, which helps in the follower prediction but limits practical application. Another advantage of SEA's over direct drive actuators is that they do not have chatter when in contact from a stiff load cell reading in high gain feedback [21]. This is an important distinction further investigated in simulation, as this sensing method is implemented most often for teleoperation. Moreover, gain limitations affect the amount of modeling error the system can handle with an SP as discussed above.

### 5.1. Simulation setup

To further investigate how the contact dynamics affect the system, a simulation was carried out in MATLAB for a generalized scenario of a 0.1 m rod making contact with a wall 0.05 m away. Actuation with a stiff motor was compared to a rotary force sensing SEA with dynamics defined by Eq. (9) with parameters listed in Table 1. Unilateral contact dynamics were implemented using the nonlinear Hunt–Crossley (HC) model [31]. The HC method is well known and widely used to model contact with viscoelastic materials [32,33]. The benefit of the HC model is that the normal force  $F_N$  is continuous and takes into account viscous friction forces for elastic conditions based on contact pseudo penetration  $\delta$ . Here the normal force is expressed as

$$F_N = K_e \delta^n + \chi \delta^n \dot{\delta}, \quad \delta(t) \geq 0. \quad (14)$$

$K_e$  is the effective stiffness calculated as

$$K_e = \frac{4\sqrt{R_i}}{3(\sigma_i + \sigma_j)} \quad (15)$$

where  $\sigma_* = (1 - \nu_*^2)/E_*$ , for  $*$  =  $i, j$ , where  $\nu_*$  and  $E_*$  is the Poisson ratio and Young's modulus respectively, for object  $i$  coming into contact with object  $j$ .  $\chi$  is the hysteresis damping factor given by [34] as

$$\chi = \frac{3K_e(1 - c_r)}{2\delta^{(-)}} \quad (16)$$

where  $c_r$  is the coefficient of restitution and  $\delta^{(-)}$  is the initial contact velocity. Contact with both a stiff and soft wall was investigated by changing  $K_e$  and  $c_r$ , as both are inversely proportional to damping [35].

### 5.2. Results and discussion

Results for contact with a stiff environment are depicted in Fig. 4 for  $K_e$  and  $c_r$  values of  $2.8 \times 10^9$  and 0.75 respectively, with a proportional gain  $K_p$  of 7.5. The target force was set to 2.5 N. The results show a

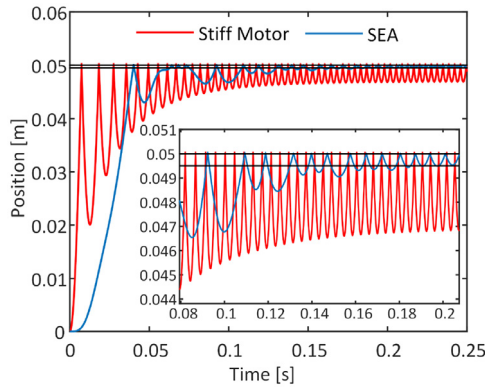


Fig. 4. SEA vs. Stiff Motor simulation results in force control with stiff unilateral contact force modeling.

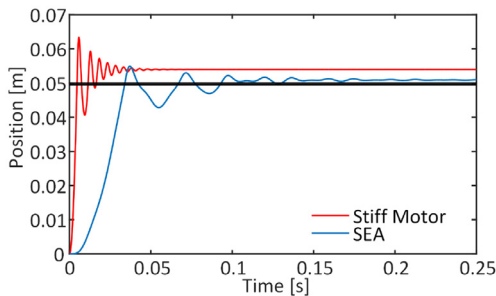


Fig. 5. SEA vs. Stiff Motor simulation results in force control with soft unilateral contact force modeling.

substantial amount of chatter and overshoot for the stiff motor, whereas the SEA settles much faster within the acceptable error.

The simulation was repeated for contact with a soft wall with  $K_e$ ,  $c_r$ , and  $K_p$  values of  $2.8 \times 10^4$ , 0.5, and 18. As the wall stiffness decreases, the SEA loses its compliance advantage and has a larger settling time than the motor as demonstrated in Fig. 5. It should be noted that because of the compliance and damping of the material, the motor settles behind the nominal contact location as the wall is deformed. Moreover, because of the SEA compliance the final settling distance within the wall is different despite having a negligible difference in steady state error.

In the proposed F-P architecture, the follower is position controlled. Simulations were also run for stiff and soft contact with proportional position control targeting the wall location at 0.05 m. The same  $K_e$  and  $c_r$  were used as before with  $K_p$  set to 80. Results did not vary much for stiff and soft contact, and are shown in Fig. 6. In both cases the stiff motor had large overshoot and chatter, but occurring with much less frequency than in the force control case. The SEA showed less overshoot than with force control. These results support the use of an SEA over a stiff motor for sensing and actuation as a means to increase the capabilities of delayed teleoperation systems.

## 6. Experimental validation

Experiments were set up to validate that the performance of a time delayed system is improved by the use of an SEA, as well as demonstrate the capability to adapt to a varying environment. A Geomagic Touch haptic device was used as the master and a force sensing SEA as the follower. For the experiment, a one degree of freedom contact task was performed for ease of comparison with literature. The Geomagic Touch user input and haptic feedback was restricted to motion along one axis. The linear actuator on the follower side used a potentiometer for position feedback to implement the Smith predictor architecture from Fig. 2.

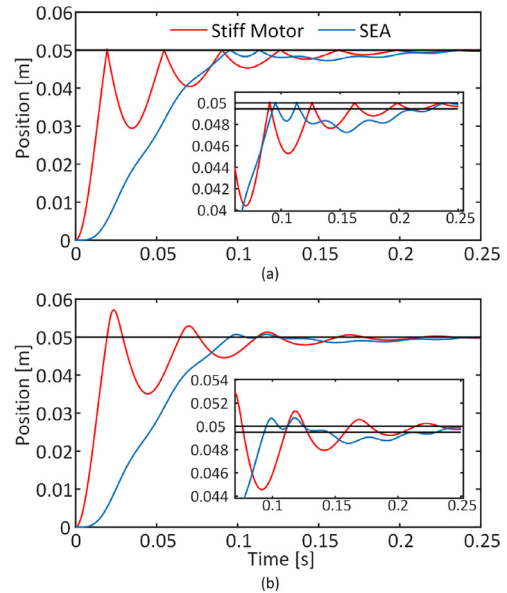


Fig. 6. SEA vs. Stiff Motor simulation results in position control with (a) stiff and (b) soft unilateral contact force modeling.

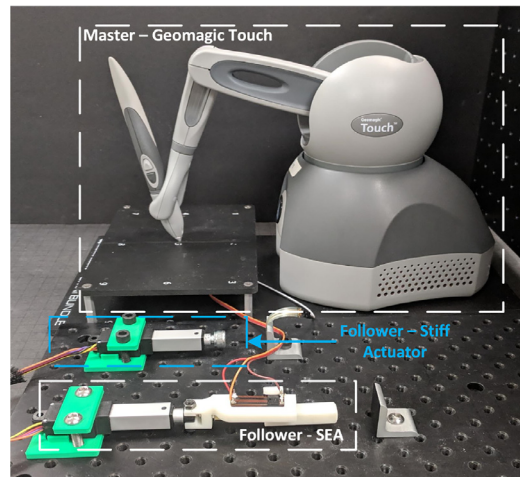


Fig. 7. Experimental setup with Geomagic Touch, SEA, and stiff actuator.

The master side control was executed on a computer communicating through a serial port to a Teensy 3.2 microcontroller on the follower side. Although serial communication does not provide a constant delay, buffer sizes were set to achieve a maximum upper bound to the delay. The master side was implemented using Simulink, and a delay block was used to create a well controlled artificial delay. The Simulink model was executed at 1 kHz. The contact experiment was conducted for a 0.5, 1, and 2 s RTT. Contact with an aluminum wall was performed with a user input target force of around 2.5 N. The estimated force signal was displayed on the computer screen to aide the user. Contact was initiated for approximately two seconds and the device was returned to the starting position to repeat the contact. The experiment was conducted with an SEA in both a stationary and varying environment. A similar test was conducted for soft contact with foam.

### 6.1. SEA contact with stiff wall

The follower uses a Firgelli L12-30-210-6-P linear actuator with a guided compression spring and a 20 kOhm linear potentiometer for the spring displacement measurement. The spring has an overall length of

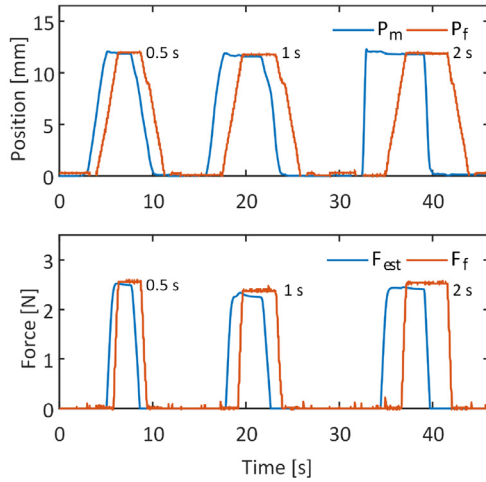


Fig. 8. Master and follower contact with an aluminum bracket for a 0.5, 1, and 2 s RTT.

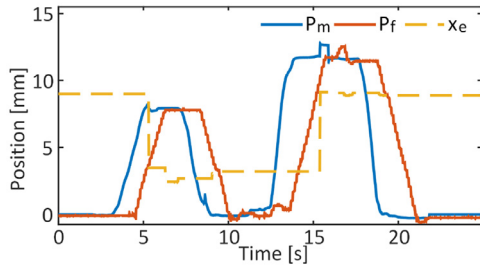


Fig. 9. Example of master and follower position with a changing environment contact location in one second RTT.

one inch and a stiffness of 0.86 N/mm (4.93 lbf/in). This size was chosen to investigate finer movements while staying within typical hand exoskeleton limits of 10 N [36]. The SEA was placed 9 mm from an aluminum L-bracket acting as the stiff wall. The environment contact position was known to the controller, and system identification was used to obtain a model for the SEA. A manually tuned PID controller was used on the follower to track the master position.

From Fig. 8 it can be seen that the use of an SEA greatly increases performance in terms of transparency for position and force tracking. These results can be compared to existing work in the field that use a stiff follower as referenced in Section 2. One of the greatest benefits of this implementation is that accurate force matching is achieved without sacrificing position accuracy as with traditional methods. With the use of an SEA, position and force is linearly related and thus the follower position tracking is also part of the environment sensing and force reflection estimation. Consequently, any position errors from inaccurate modelling of the follower and environment dynamics will directly affect the force tracking. Additionally, from a more detailed inspection of Fig. 8, the resolution of the spring displacement affects the force reflection accuracy since the force and displacement are coupled in an SEA. However, the proposed system still demonstrates excellent performance, with force reflection accuracy to within a few tenths of a Newton, and position tracking to less than half a millimeter, even at a time delay of two seconds. Some data packet losses were observed, but the occurrence was infrequent and did not have any significant effects on performance.

## 6.2. Varying environment and soft contact

In most studies, the environment is assumed to be stationary, and determining the contact location is often overlooked or assumed to be known a priori. This is one of the greatest limitations to practical ap-

Table 2  
Varying environment contact location error.

RTT [s]	3 mm Contact [mm]	
	max dev.	avg. settling dev.
0.5	0.688	0.336
1.0	0.647	0.393
2.0	0.534	0.522
RTT [s]	9 mm Contact [mm]	
	max dev.	avg. settling dev.
0.5	0.186	0.102
1.0	0.209	0.097
2.0	0.094	0.102

plication of teleoperation systems since environments in real life are often time varying. Based on a review of recent work, few studies have mentioned the capability to handle varying contact positions [5,13], with limited discussion. However, the ability to adapt to time varying environments is important to extend the capabilities of teleoperation, particularly in the presence of time delay.

An experiment was conducted where the environment contact sensing and correction (ECSC) method defined in Eq. (13) was applied to the SEA controller. A 6 mm block was placed between the wall and the SEA to change the contact location. The user was instructed to make contact with the wall as before, assuming the original contact location at 9 mm. The teleoperation system was set with an initial contact location of 9 mm as well. After the first contact, the block was removed and the user was instructed to make a second contact at the original wall location at 9 mm.

The ECSC is an online correction method that is constantly executed throughout the motion. However, because it is based on  $F_f$ , it is only updated once contact is initiated. Moreover, since the ECSC is on the follower side, the user receives an update only after the backwards time delay duration, or half the RTT for a constant and symmetric delay as in this implementation. The accuracy of the sensing method is affected by the model accuracy and position error. As before, the SEA spring displacement resolution also has an effect on the ECSC and thus an appropriate sensor must be selected for the specific application of the teleoperation system.

Knowledge of the contact location is necessary for predictive approaches based on an SP, and affects the force sensing of the SEA. As such, this becomes critical information for the proposed teleoperation architecture. To evaluate the performance of the ECSC the test was conducted with five trials at RTT's of 0.5, 1, and 2 s. The maximum deviation and average settled value after contact is shown in Table 2. The results do not follow any significant trend, although the average settled  $x_e$  error was larger for trials with a two second time delay. This is likely due to the increasing error between  $F_f$  and  $F_p$  as the communication delay increases, causing drift between the estimated  $x_e$  and the actual contact location. This provides the first quantitative result known to the authors for capabilities to compensate for environment variations. Contact tests were also conducted with a soft environment using a foam block. For soft materials the contact location changes as the material deforms. Therefore,  $x_e$  must be updated on the master side to prevent modelling errors that will degrade performance and potentially destabilize the system. Fig. 10 demonstrates the performance of the proposed system and the ability of the ECSC to correct for dynamic environment variations on top of the static case discussed above.

For small time delays, the ECSC is able to correct  $G'_p$  with small force errors. As the delay increases, the update time causes greater force estimation overshoot until contact is maintained and the correction allows  $F_{est}$  and  $F_f$  to converge. Although in dynamic environment variation the correction will always trail the actual contact location, in small delays the performance can be acceptable for small bandwidths. More-

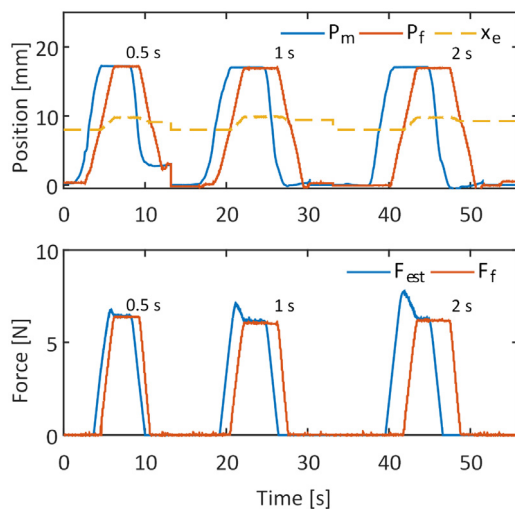


**Fig. 10.** Master and follower contact with foam block environment location, 0.5, 1, and 2 s RTT.

over, these results are particularly promising as the ECSC assumes no knowledge of the environment dynamics.

## 7. Conclusion

This work presented the improvement in performance and transparency for a robust teleoperation system with the use of an SEA on the follower side in a F-P architecture using a Smith predictor. Simulation results demonstrate the benefit of using an SEA for unilateral contact with a stiff environment over direct actuation. Compliance in the system demonstrated a reduction in chatter and overshoot for both force and position control in stiff and soft environments. In experiment, accurate force and position tracking was achieved in an RTT of two seconds for contact with a stiff environment. Additionally, a method to account for variations in contact location, ECSC, was developed and demonstrated. Contact with a soft environment showed good performance in an RTT delay of 500 ms.

The results provide promising direction for increasing teleoperation performance further as part of future work. Currently, the proposed system assumes no knowledge of the environment dynamics, and takes advantage of the coupled actuation and sensing capabilities of the SEA. Estimation of the follower-environment dynamics can be added to the control architecture to improve the follower side prediction. This has the potential to reduce the update error in the ECSC as well, resulting in better performance in the presence of increased delays for soft contact. This would be particularly useful in telesurgery applications for interacting with soft tissue. This work can also be extended by extending it to a multi-degree of freedom manipulator, as evaluating specific task performance and completion times will be a useful metric to further evaluate the system's practical application.

## Declaration of Competing Interest

The authors declare that they have no known competing financial interests or personal relationships that could have appeared to influence the work reported in this paper.

## Acknowledgments

This work was supported in part by the US Army Medical Research & Materiel Command's Telemedicine and Advanced Technology Research Center (TATRC), under Contract no. W81XWH-16-C-0062. The views, opinions, and/or findings contained in this paper are those of the authors and should not be construed as an official Department of the

Army position, policy, or decision unless so designated by other documentation. The author would like to thank Bijo Sebastian and Raghuraj Chauhan for their support in this work.

## References

- [1] Uddin R, Ryu J. Predictive control approaches for bilateral teleoperation. *Annu Rev Control* 2016;42:82–99. doi:10.1016/j.arcontrol.2016.09.003.
- [2] Hokayem PF, Spong MW. Bilateral teleoperation: an historical survey. *Automatica* 2006;42(12):2035–57. doi:10.1016/j.automatica.2006.06.027.
- [3] Rui Cortesao, Jaeheung Park, Khatib O. Real-time adaptive control for haptic manipulation with active observers. In: *Proceedings 2003 IEEE/RSJ international conference on intelligent robots and systems (IROS 2003)* (Cat. No. 03CH37453), 3. IEEE; 2003. p. 2938–43. ISBN 0-7803-7860-1. doi:10.1109/IROS.2003.1249317.
- [4] Hosseini-Suny K, Momeni H, Janabi-Sharifi F. Model reference adaptive control design for a teleoperation system with output prediction. *J Intell Robot Syst* 2010;59(3–4):319–39. doi:10.1007/s10846-010-9400-4.
- [5] Smith AC, Hashtrudi-Zaad K. Smith predictor type control architectures for time delayed teleoperation. *Int J Robot Res* 2006;25(8):797–818. doi:10.1177/0278364906068393.
- [6] Choi HJ, Jung S. Neural network-based smith predictor design for the time-delay in a tele-operated control system. *Artif Life Robot* 2009;14(4):578–83. doi:10.1007/s10015-009-0750-6.
- [7] Lee D, Spong M. Passive bilateral teleoperation with constant time delay. *IEEE Trans Robot* 2006;22(2):269–81. doi:10.1109/TRO.2005.862037.
- [8] Mima K, Honda M, Miyoshi T, Imamura T, Okabe M, Yazadi FM, et al. Telem Manipulation with a humanoid robot hand/arm between USA and Japan. In: *2013 IEEE international conference on robotics and automation. IEEE*; 2013. p. 3618–24. ISBN 978-1-4673-5643-5. doi:10.1109/ICRA.2013.6631085.
- [9] Seo C, Kim J-P, Kim J, Ahn H-S, Ryu J. Robustly stable bilateral teleoperation under time-varying delays and data losses: an energy-bounding approach. *J Mech Sci Technol* 2011;25(8):2089–100. doi:10.1007/s12206-011-0523-8.
- [10] Uddin R, Park S, Ryu J. A predictive energy-bounding approach for haptic teleoperation. *Mechatronics* 2016;35:148–61. doi:10.1016/j.mechatronics.2016.02.003.
- [11] Yang Y, Li H, Chen Y, Yi J. Model predictive control for space teleoperation systems based on a mixed-H2/happroach. *J Aerosp Eng* 2015;28(5):04014133. doi:10.1061/(ASCE)AS.1943-5525.0000469.
- [12] SMITH, M OJ. Closed control of loop with dead time. *Chem Eng Prog* 1957;53:217–19.
- [13] Chan L, Naghdy F, Stirling D. Position and force tracking for non-linear haptic telemanipulator under varying delays with an improved extended active observer. *Robot Auton Syst* 2016;75:145–60. doi:10.1016/j.robot.2015.10.007.
- [14] Kim W, Hannaford B, Fejczy A. Force-reflection and shared compliant control in operating telemanipulators with time delay. *IEEE Trans Robot Autom* 1992;8(2):176–85. doi:10.1109/70.134272.
- [15] Lawrence D. Stability and transparency in bilateral teleoperation. *IEEE Trans Robot Autom* 1993;9(5):624–37. doi:10.1109/70.258054.
- [16] Anderson R, Spong M. Bilateral control of teleoperators with time delay. *IEEE Trans Autom Control* 1989;34(5):494–501. doi:10.1109/9.24201.
- [17] Niemeyer G, Slotine J-JE. Telem Manipulation with time delays. *Int J Robot Res* 2004;23(9):873–90. doi:10.1177/0278364904045563.
- [18] Yang Y, Hua C, Guan X. Finite time control design for bilateral teleoperation system with position synchronization error constrained. *IEEE Trans Cybern* 2016;46(3):609–19. doi:10.1109/TCYB.2015.2410785.
- [19] Whitney DE. Quasi-static assembly of compliantly supported rigid parts. *J Dyn Syst Meas Control* 1982;104(1):65. doi:10.1115/1.3149634.
- [20] Pratt GA, Williamson MM, Dillworth P, Pratt J, Wright A. Stiffness isn't everything. In: *Experimental robotics IV*. London: Springer-Verlag; 1995. p. 253–62. ISBN 978-3-540-76133-4. doi:10.1007/BFb0035216.
- [21] Pratt J, Krupp B, Morse C. Series elastic actuators for high fidelity force control. *Ind Robot* 2002;29(3):234–41. doi:10.1108/01439910210425522.
- [22] Bodie K, Bellicoso CD, Hutter M. ANYpulator: design and control of a safe robotic arm. In: *2016 IEEE/RSJ International Conference on Intelligent Robots and Systems (IROS)*. IEEE; 2016. p. 1119–25. ISBN 978-1-5090-3762-9. doi:10.1109/IROS.2016.7759189.
- [23] Aiple M, Schiele A. Towards teleoperation with human-like dynamics: Human use of elastic tools. In: *2017 IEEE World Haptics Conference (WHC)*. IEEE; 2017. p. 171–6. ISBN 978-1-5090-1425-5. doi:10.1109/WHC.2017.7989896.
- [24] King C-H, Killpack MD, Kemp CC. Effects of force feedback and arm compliance on teleoperation for a hygiene task. In: *Lecture notes in computer science (including subseries lecture notes in artificial intelligence and lecture notes in bioinformatics)*, 6191; 2010. p. 248–55. ISBN 3642140637. doi:10.1007/978-3-642-14064-8\_36. LNCS
- [25] Hua C-C, Yang X, Yan J, Guan X-P. On exploring the domain of attraction for bilateral teleoperator subject to interval delay and saturated p + d control scheme. *IEEE Trans Autom Control* 2017;62(6):2923–8. doi:10.1109/TAC.2016.2603780.
- [26] Munir S, Book W. Internet-based teleoperation using wave variables with prediction. *IEEE/ASME Trans Mechatron* 2002;7(2):124–33. doi:10.1109/TMECH.2002.1011249.
- [27] Fraisse P, Lelevé A. Teleoperation over IP network: network delay regulation and adaptive control. *Auton Robot* 2003;15(3):225–35. doi:10.1023/A:1026112419614.
- [28] Kamrani E. Real-time internet-based teleoperation. *Intell Control Autom* 2012;03(04):356–75. doi:10.4236/ica.2012.34041.
- [29] Ganjefar S, Momeni H, Janabi Sharifi F, Hamidi Beheshti M. Behavior of Smith predictor in teleoperation systems with modeling and delay time errors. In: *Proceedings*

- of 2003 IEEE conference on control applications, 2003. CCA 2003., 2. IEEE; 2003. p. 1176–80. ISBN 0-7803-7729-X. doi:[10.1109/CCA.2003.1223177](https://doi.org/10.1109/CCA.2003.1223177).
- [30] Lee C, Kwak S, Kwak J, Oh S. Generalization of series elastic actuator configurations and dynamic behavior comparison. *Actuators* 2017;6(3):26. doi:[10.3390/act6030026](https://doi.org/10.3390/act6030026).
- [31] Hunt KH, Crossley FRE. Coefficient of restitution interpreted as damping in vibroimpact. *J Appl Mech* 1975;42(2):440. doi:[10.1115/1.3423596](https://doi.org/10.1115/1.3423596).
- [32] Haddadi A, Hashtrudi-Zaad K. Real-time identification of Hunt Crossley dynamic models of contact environments. *IEEE Trans Robot* 2012;28(3):555–66. doi:[10.1109/TRO.2012.2183054](https://doi.org/10.1109/TRO.2012.2183054).
- [33] Pappalardo A, Albakri A, Liu C, Bascetta L, De Momi E, Pognet P. Hunt Crossley model based force control for minimally invasive robotic surgery. *Biomed Signal Process Control* 2016;29:31–43. doi:[10.1016/j.bspc.2016.05.003](https://doi.org/10.1016/j.bspc.2016.05.003).
- [34] Flores P, Lankarani HM. Contact force models for multibody dynamics. *Solid Mechanics and Its Applications*, 226. Cham: Springer International Publishing; 2016. ISBN 978-3-319-30896-8. doi:[10.1007/978-3-319-30897-5](https://doi.org/10.1007/978-3-319-30897-5).
- [35] Jacobs DA, Waldron KJ. Modeling inelastic collisions with the Hunt Crossley model using the energetic coefficient of restitution. *J Comput Nonlinear Dyn* 2015;10(2):021001. doi:[10.1115/1.4028473](https://doi.org/10.1115/1.4028473).
- [36] Refour E, Sebastian B, Ben-Tzvi P. Two-digit robotic exoskeleton glove mechanism: design and integration. *J Mech Robot* 2018;10(2):025002. doi:[10.1115/1.4038775](https://doi.org/10.1115/1.4038775).



**Daniel Budolak** received his B.S. degree in Mechanical Engineering from the University of Illinois at Chicago in 2016. He is currently a Masters student with research interests in mechatronics and robotics, particularly in space applications.



**Pinhas Ben-Tzvi** (S'02-M'08-SM'12) received the B.S. degree (summa cum laude) in mechanical engineering from the Technion-Israel Institute of Technology, Haifa, Israel, in 2000 and the M.S. and Ph.D. degrees in mechanical engineering from the University of Toronto, Toronto, ON, Canada, in 2004 and 2008, respectively. He is currently an Associate Professor of Mechanical Engineering and Electrical and Computer Engineering, and the founding Director of the Robotics and Mechatronics Laboratory at Virginia Tech, Blacksburg, VA, USA. His current research interests include robotics and intelligent autonomous systems, human-robot interactions, robotic vision and visual servoing/odometry, machine learning, mechatronics design, systems dynamics and control, mechanism design and system integration, and novel sensing and actuation. Dr. Ben-Tzvi is the recipient of the 2019 Virginia Tech Excellence in Teaching Award, 2018 Virginia Tech Faculty Fellow Award, the 2013 GWU SEAS Outstanding Young Researcher Award and the GWU SEAS Outstanding Young Teacher Award, as well as several other honors and awards. Dr. Ben-Tzvi is Technical Editor for the IEEE/ASME Transactions on Mechatronics, Associate Editor for ASME Journal of Mechanisms and Robotics, Associate Editor for IEEE Robotics and Automation Magazine, and an Associate Editor for the Int'l Journal of Control, Automation and Systems and served as an Associate Editor for IEEE ICRA 2013, 2014, 2016, 2017, and 2018. He is a member of the American Society of Mechanical Engineers (ASME).